Engineering and Technology Journal
Journal homepage: https://etj.uotechnology.edu.iq

Investigating the effect of spray parameters on adhesion strength between aluminum coatings and polymeric substrate

Ghufran J. Matrood*, Niveen J. Abdulkader, Nahedh M. Ali

Materials Engineering Dept., University of Technology-Iraq, Alsina'a street, 10066 Baghdad, Iraq.
*Corresponding author Email: mae.19.41@grad.uotechnology.edu.iq

HIGHLIGHTS

- Metallic coatings on HDPE substrates were studied using the flame thermal spray technique.
- The effect of thermal spray parameters on adhesion strength was investigated.
- Metallic powder enabled successful coating without damaging the polymeric substrate.

ARTICLE INFO

Handling editor: Akram R. Jabur

Keywords:

Thermal spray

Aluminum

HDPE

Electrical conductivity

Taguchi methodology

ABSTRACT

Metallization involves applying a thin metal layer onto a substrate, typically through techniques such as thermal spraying. This process improves conductivity, durability, and aesthetic appeal, making it valuable in applications such as electronics, solar panels, and decorative coatings. In this study, flame thermal spray technique are used to metalize high-density polyethylene with an aluminum layer. Taguchi and ANOVA are used to investigate the effect of various parameters on the adhesion strength between aluminum layers deposited on high-density polyethylene (HDPE) substrates. DOE utilization has facilitated the identification of the effects of the flame thermal spraying parameters, such as the distance between the spray gun and substrate, the spray velocity, the powder feed rate, and the delay time, on the adhesion strength. The orthogonal matrix resulting from the Taguchi method corresponded to an L9 (34) matrix, which was utilized to decrease the number of experiments from 81 to 9. To attain optimal adhesion strength, it is essential to maintain a distance of 250 mm between the gun spray and the substrate, utilize a powder feeding rate of 15 g/minute, achieve a spraying velocity of 300 m/min, and implement a delay time of four minutes. The X-ray diffraction shows that there is no oxidation in the coating layer. Moreover, the aluminum layer shows good electrical conductivity (2.08×10^4 $\Omega^{-1}.cm^{-1}$). Using Taguchi and ANOVA leads to optimizing processes efficiently with fewer trials, improving product quality by reducing variability, and making informed decisions on which factors to control for optimal performance.

1. Introduction

Polymer metallization is an emerging area of study that aims to combine the advantageous features of metal coatings with those of plastic substrates [1-4]. In this context, the materials used for a wide range of contemporary manufactured products are selected based on the characteristics that make them suitable for the intended purpose of the products. In particular, polymers exhibit both corrosion resistance and resistance to a wide range of common chemicals and are also lightweight. However, they lack the hardness of metals and have low thermal and electrical conductivity [5]. The numerous applications of metallized polymers range from microelectronics to food packaging [6,7].

To this end, thermal spraying is a process where a molten or partially molten material is applied to a surface using a high-velocity spray to create a coating. When the coating particles come into contact with the substrate surface, they undergo permanent deformation, forming a coating layer. The coating material can be employed in either a powder or wire form. In this regard, oxygen and acetylene (C_2H_2) are the gases used to generate heat in flame thermal spray. When exposed to heat, the coating material melts quickly and is forcefully released onto the surface of the substrate [8-10].

Nanomaterials are viewed as profoundly impacting almost every facet of human existence. This effect has the potential to significantly impact numerous domains, including physical sciences, biotechnology, energy, communication technology, social psychology, manufacturing, catalysis, computational sciences, and transportation. In addition, this innovation can significantly transform the future by improving the durability and reactivity of existing materials [11-13]. In particular, metal nanoparticles are nanomaterials composed of a single element. Single atoms or clusters of many atoms may occur. In this regard, gold, silver,

http://doi.org/10.30684/etj.2024.155226.1850
Received 15 November 2024; Received in revised form 19 December 2024; Accepted 22 December 2024; Available online 26 December 2024
2412-0758/University of Technology-Iraq, Baghdad, Iraq

platinum, copper, palladium, rhenium, zinc, ruthenium, cobalt, cadmium, aluminum, nickel, and iron are among the most frequently synthesized nanoparticles [14]. Specifically, aluminum (Al) nanoparticles exhibit distinctive optical, physical, and chemical properties, positioning them as suitable candidates for diverse applications, including nanophotonic, catalysis, and the development of higher energy composite. The chemical and physical properties of Al, particularly its nanoparticles, render them suitable for diverse applications, which include alloy powder metallurgy components for automobiles and aircraft, heat shielding coatings for aircraft, corrosion-resistant and conductive coatings, heat-reflective coatings, conductive and decorative plastics, soldering and termite welding, as well as uses in pyrotechnics and military applications, such as rocket fuel, igniters, smoke devices, and tracers. In particular, nanoscale aluminum particles are investigated for their potential as high-capacity hydrogen storage materials [15,16].

Polymers have been pivotal in advancing technology, applied engineering, and materials throughout history. They have replaced their metallic equivalents in several applications, including medicine, construction, energy, water treatment, and electronics. This feature results from low material and processing costs, extensive elasticity, strength, conductivity, degradability, and adaptability to increasingly intricate production methods [17]. High-density polyethylene, often called HDPE, is the plastic industry's most frequently used non-crystalline substance. Mainly, HDPE is stiff and resistant to heat and abrasion. Under free-radical polymerization, the procedure uses trace quantities of oxygen or peroxide (benzoyl or diethyl). Sometimes, the starting agents are azo and hydroperoxide compounds [18].

Design of experiments (DOE) is an effective method that streamlines and reduces the number of necessary tests for system optimization, resulting in a substantial decrease in time. It comprises an experimental approach that concurrently examines the influence of many variables at numerous levels [19,20]. In this method, factors are defined as the variables that directly impact the process under investigation, while levels are the values that these factors assume throughout trials. This approach constructs an orthogonal array delineating the required experiments to conduct. In this context, the analysis of variance (ANOVA) is used to ascertain the response magnitude of each variable (in %) inside the orthogonal array [21,22]. Taguchi's design of experiments (DOE) methodology is accessible and applicable for users with modest statistical expertise, making it a popular choice in the fields of engineering and science [23-26].

Voyer et al. [27], utilized cooling air to lower the temperature of a polymer substrate employed in deposition via flame spraying. The findings indicated that employing cooling air and modifying spraying parameters facilitates a reduction in the distance between the flame torch and the substrate, successfully preventing thermal damage to the polymer substrate, which is a fact that can be readily verified through visual inspection. Flame-sprayed coatings can affect the electrical properties of a polymer substrate, regardless of the possible implications of the deposition method on the structural integrity of the applied coatings. Ashrafizadeh et al. [28], utilized compressed air, resulting in a reduction of the electrical resistance of the coating, which is associated with a decrease in the porosity of the Al-12Si layer due to the increase. Compressed air improves the impact velocity of the sprayed particles, resulting in enhanced deformation characteristics. To ensure a stable substrate temperature, it is advisable to decrease the distance between the substrate and the spray gun in conjunction with raising both the ejection pressure and the flow rate of the compressed air. Reducing the distance between the substrate and the spray gun is essential for obtaining thick layers of Al-12Si. Huonnic et al. [29], measured the electrical resistance of flame-sprayed glass and basalt tubes after a layer of aluminum coating was deposited on the surface, which was found to be 69×10^7 Ω.cm and 89×10^7 Ω.cm, respectively. Two flame sprayers produced a uniform metal layer with electrical properties on a polymeric substrate. It was noted that the electrical resistance values of the coated materials were higher than those of the annealed aluminum alloy. Affi et al. [30], analyzed the electrical resistance of Al coatings applied by cold and plasma spraying methods onto carbon-fiber-reinforced epoxy substrates. The resistance values of the aluminum deposits sprayed with plasma were significantly higher than those of the aluminum coatings sprayed with a low temperature. This outcome could be attributed to the increased oxidation of the sprayed particles at higher carrier gas temperatures. Mohammed et al. [31], studied the effect of flame thermal spray parameters (stand-off distance, powder feed rate, transverse velocity, and delay time) on the deposition efficiency of the Al layer using Taguchi and ANOVA. The findings affirmed that the stand-off distance was the most influential factor in the FSTC process, followed by powder feed rate, the time of one spray, and transverse velocity.

A review of the existing literature revealed that the challenges associated with the metalizing process, which results in the deformation of polymers during the coating procedure, have been thoroughly examined. This study will tackle these challenges by utilizing compressed air to reduce excessive heat on the polymer substrate, which leads to polymer deformation and the resulting weakening of adhesion between the coating layer and the polymer substrate material. Specifically, the samples were coated under different conditions, and the Taguchi method was used to find the optimal conditions for obtaining the best adhesion between the substrate material and the coated layer. Using Taguchi and ANOVA leads to optimizing processes efficiently with fewer trials, improving product quality by reducing variability, and making informed decisions on which factors to control for optimal performance.

The main motivations for using metallized polymers in producing electronic devices are to reduce costs, decrease weight, and enhance electrical conductivity. In this study, HDPE polymers were metalized with Al to obtain lightweight products with electrical conductivity and a reasonable adhesion force between the polymer substrate and the metallic coating.

2. Experimental work

2.1 Materials

High-density polyethylene (HDPE) 3×2 cm^2 was used as the substrate material, and Al nanoparticle powder was used as the coating material. The aluminum utilized in this study was sourced from NRE/India, featuring a purity of 99% and a particle size of 61.8 nm. The chemical composition and particle size of the Al powder are presented in Table (1). The particle size of Al was examined using a laser diffraction particle size distribution analyzer. The test was conducted at the Nanotechnology and Advanced Materials Research Center / University of Technology, and the Ministry of Science and Technology examined the chemical composition.

Table 1: The chemical composition of pure Aluminum

Element%	Ti	Zn	Cu	Fe	Mn	Si	V	Mg	Al
Composition	0.024	0.033	0.026	0.15	0.045	0.052	0.008	0.028	Balance

2.2 The coating process

Initially, HDPE substrates underwent a cleaning process utilizing NaOH before the commencement of the coating procedure. Subsequently, sandpaper created a roughened texture on the substrate material. Two torch flame spray devices were employed in the coating process following the cleaning and roughening of the HDPE substrates. In particular, the procedure consists of introducing aluminum particles into the flame until they reach a molten state, followed by the application of compressed air to atomize the semi-molten aluminum particles, which were subsequently deposited onto the polymeric substrate, resulting in the formation of an aluminum top coat on the surface of the HDPE substrates. The required velocity was achieved utilizing combustion gases and/or auxiliary compressed air. Moreover, the partial pressure of O_2 was measured at 0.5 bar, while the partial pressure of C_2H_2 was recorded at 1 bar [32]. In addition, air cooling was utilized to avert the polymer's deterioration and improve the adhesion strength between the polymeric substrate and the metallic coating. Figures (1 and 2) depict the two torch flame spray devices alongside the samples before and after the coating procedure.

Figure 1: The two torch flame spray devices

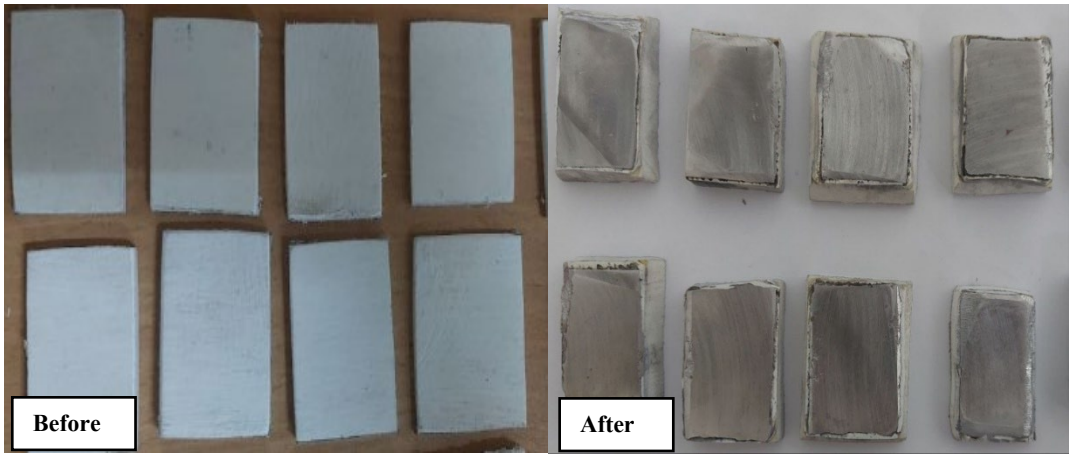

Figure 2: Images of the samples before and following the coating

3. Design of experiment, characterization, and tests

An experimental investigation was conducted to determine the optimum flame thermal spray parameters utilizing the design of experiments. The Taguchi methodology, specifically L9 orthogonal arrays, was employed in the Minitab 17 software. Tables (2 and 3) present four parameters along with their respective levels.

Table 2: Thermal spraying factors and their levels

Factor	Distance (mm)	Powder feed rate (g/min)	Spraying velocity (m/min)	Delay time (min)
Level (1)	150	15	100	4
Level (2)	200	30	200	6
Level (3)	250	40	300	8

Table 3: The Taguchi orthogonal array

No. of Experiments	1	2	3	4	5	6	7	8	9
Distance (mm)	150	150	150	200	200	200	250	250	250
Powder feeding (g/ min)	15	30	45	15	30	45	45	15	30
Spray velocity (m/min)	100	200	300	200	300	100	100	300	200
Delay time (min)	4	6	8	8	4	6	6	8	4

To determine the optimal factor affecting the thermal spraying process using DOE, the following steps must be followed: define the goal (outputs), identify the factors that are believed to be influential in determining the goal, enter the level for each of the factors (the distance between the substrate and spray gun, the spray velocity, powder feeding, and delay time) to the program (Minitab 17), the program will create the matrix and analyzes the data contained in the matrix and creates main effect plot for mean and S/N Ratio, finally using ANOVA technique to analyze data more accurately, where the effect of two factors on the target is studied.

A contact angle test is a widely utilized method for assessing the wettability of a surface or substance. The contact angle is formed at the intersection of the liquid-solid and liquid-vapor interfaces [33]. The wetting phenomenon pertains to how a liquid disperses over a solid surface or the capacity of a liquid to establish an interface with a solid entity. This work measured wettability at the Department of Chemical Engineering, University of Technology, Baghdad.

Scratch testing is the primary and favored technique for assessing the adhesive strength of a coating-substrate system [34-36]. In this test, a specimen measuring 2×3 cm^2 is firmly positioned. A sharp tip is then dragged across the material's surface while applying a controlled load, and the resulting damage is observed. The implementation of this test complies with the specifications outlined in ASTM D4541. The examination was performed at the Applied Sciences Department at the University of Technology \ Iraq. The electrical conductivity of the metallic layer was assessed using an LCR-821 meter at the Department of Materials Engineering, Technical College, Baghdad.

X-ray diffraction and scanning electron microscopy were used to characterize the metallic coating layer and the interface between the HDPE polymeric substrate and the Al metallic coating layer. The XRD was performed at the Nanotechnology and Advanced Materials Research Centre of the University of Technology \ Iraq, Baghdad, employing Shimadzu XRD 6000 X-ray diffraction equipment, and SEM in AlKora Company employing Thermo Scientific SEM equipment.

4. Results and discussion

The contact angle of the HDPE samples measured 57.227, which indicates that the surface of HDPE possesses favorable surface energy and strong adhesiveness. We can estimate the material's surface energy by measuring the contact angle of a liquid drop on a surface. This is useful in coatings and adhesion strength. The surface free energy quantifies the additional energy found at the material's surface, which can be utilized to characterize the wetting and adhesion properties between different materials [37]. This outcome means that the HDPE samples have good surface energy, and hence, the molten Al particle will spread on the HDPE substrate, forming good adhesion between the substrate and the coating layer.

The X-ray diffraction analysis of the aluminum layer on a polymer substrate exhibits similarities to those observed in a standard sample. The low peaks suggest a random or uneven coating structure, as shown in Figure (3), whereas the firm peaks with a narrow basis indicate a uniform crystal structure.

Scherrer equation was used to compute the average crystallite size as follows in Equation (1) [38]:

$$D = \frac{\lambda K}{\beta Cos\ 2\theta} \quad (1)$$

where D is the average crystallite size (nm), λ is the wavelength of the applied X-ray radiation (1.540 nm), K is the Scherrer constant (0.94), β is the full width at half maximum (FWHM) of the diffraction peak (radians), and 2Θ is Bragg angle about the peak of high intensity (2Θ = 65.04°). The average crystallite size was computed at 15 nm. The calculated average crystallite size of Al on HDPE is 253 nm, determined from the half-width of the (2 2 0) diffraction peak.

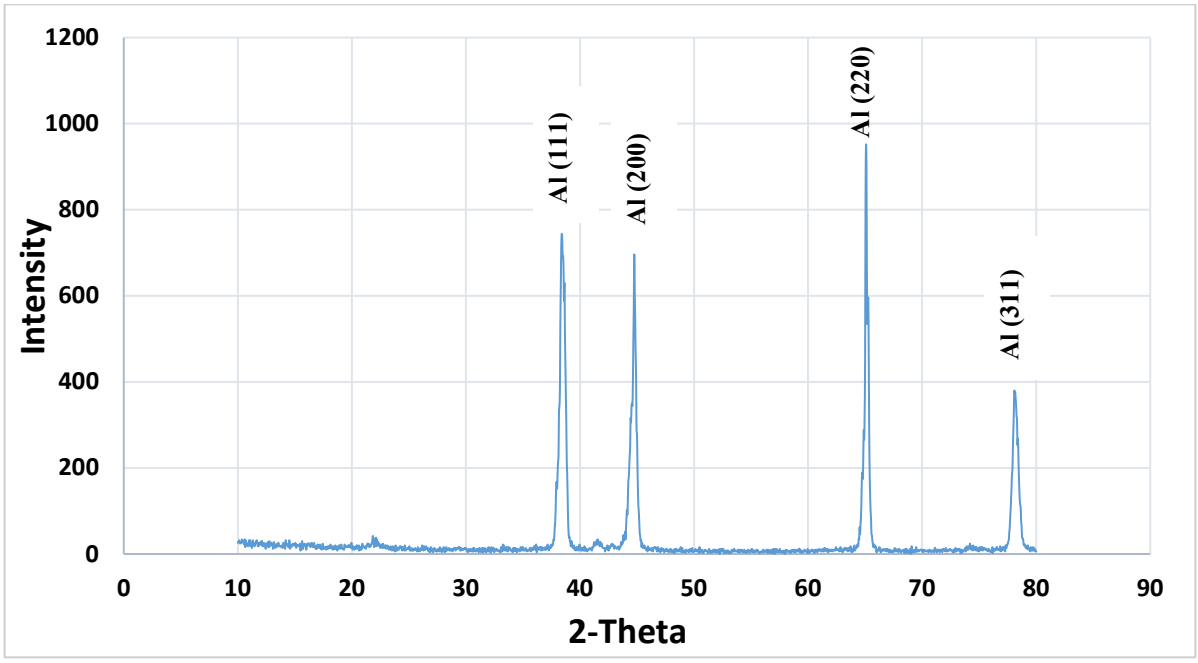

Figure 3: XRD of the Al layer on the HDPE substrate

Figure (4) illustrates the interface between the HDPE polymeric substrate and the aluminum metallic coating layer. The observation indicates that the interface between the Al metallic coating layer and the HDPE polymeric substrate remains undeformed, and there is no evidence of polymer degradation. The adhesion between the coating layer and the substrate is also strong. Moreover, the Al coating layer has a thickness of 74 µm.

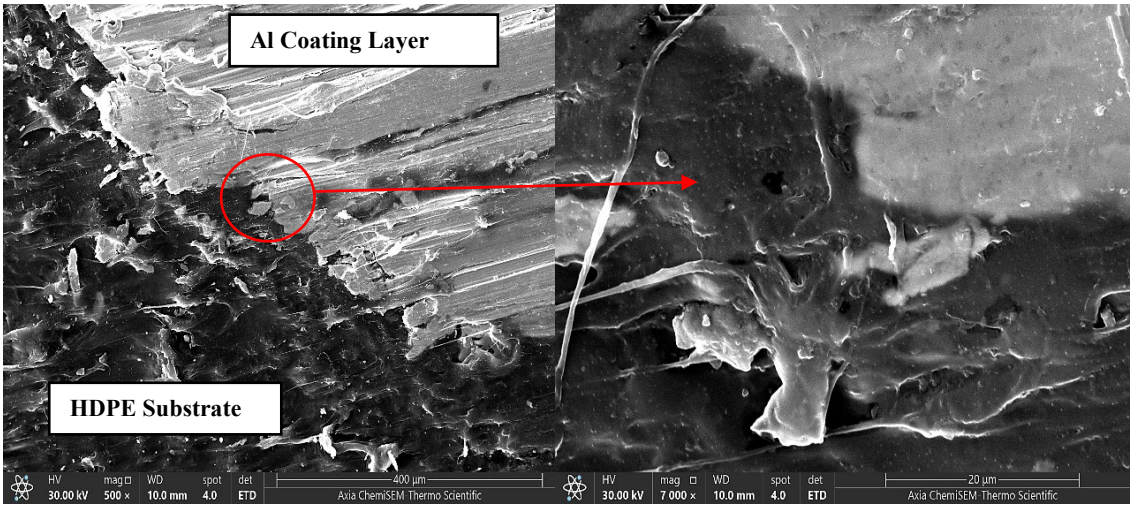

Figure 4: SEM of the interface between the Al layers on the HDPE substrate

The Al layer has an electrical conductivity of 2.08×10^{4} $\Omega^{-1}.cm^{-1}$, much lower than bulk Al's conductivity. This is because the nanoparticles in the coating layer raised the resistance values due to a rise in grain boundaries. The electrical conductivity value of bulk aluminum is measured at 3.77×10^{5} $\Omega^{-1}.cm^{-1}$. In this regard, the lower electrical conductivity of the Al coating layer compared to that of the aluminum is attributed to the presence of nanoparticles that increase the number of grain boundaries [39].

The scratch test was carried out on nine specimens. Parameters such as the distance between the substrate and spray gun, the spray velocity, powder feeding, and delay time changed at three different levels, as shown in Table (3). The same spraying conditions were used for the tests, each repeated three times to obtain better averages of the results. The data presented in Table (4) indicates that optimal adhesion can be attained by maintaining a distance of 250 millimeters between the gun spray and the substrate, a powder feeding rate of 15 g/min, a spray velocity of 300 m/min, and a delay period of six minutes.

The primary factors affecting the adhesion strength are the distance between the substrate and the spray gun, which has a high delta value of 0.6 S/N ratio and a mean of 2.7, ranking it first. The impact of the powder feeding on the adhesion strength is minimal, as indicated by a low delta value of 0.04 S/N ratio and a mean of 0.19, corresponding to Rank 4, as presented in Tables (5 and 6).

Table 4: The Taguchi orthogonal array results

No. of experiments	1	2	3	4	5	6	7	8	9
Trial 1	37.55	37.75	37.84	37.80	38.88	36.99	40.83	39.61	40.81
Trial 2	37.54	37.77	37.88	37.81	38.87	36.96	40.82	39.66	40.79
Trial 3	37.57	37.78	37.83	37.81	37.89	36.98	40.84	39.69	40.79
Mean	37.5533	37.7667	37.8500	37.8067	38.5467	36.9767	40.8300	39.6533	40.7967
S/N Ratio	31.50	31.54	31.56	31.55	31.72	31.36	32.22	31.96	32.21

Trial 1, Trial 2, and Trial 3 represent the adhesion forces measured in Newtons (N).

Table 5: Response table for the S/N Ratio

Level	1	2	3	Delta	Rank
Distance (mm)	31.53	31.54	32.13	0.6	1
Powder Feed Rate (g/min)	31.75	31.74	31.71	0.04	4
Spray Velocity (m/min)	31.61	31.77	31.83	0.23	2
Delay Time (min)	31.81	31.71	31.69	0.12	3

Table 6: Response table for mean

Level	1	2	3	Delta	Rank
Distance (mm)	37.72	37.78	40.43	2.7	1
Powder Feed Rate (g/min)	38.73	38.66	38.54	0.19	4
Spray Velocity (m/min)	38.06	38.79	39.08	1.01	2
Delay Time (min)	38.97	38.52	38.44	0.53	3

Figures (5 and 6) show the main effects plot for the means and the main effects plot for the SN ratio, respectively. More specifically, four parameters with three levels are used for each parameter. The parameters are the distance between the substrate and the spray gun (150, 200, and 250) mm, the spraying velocity (100, 200, and 300) m/min, the powder feeding (15, 30, and 45) g/min, and the delay time (4, 6, and 8) min. It explains each factor's effect on the adhesion force's output. We note that the highest adhesion force that can be obtained is at a distance of 250 mm, which is the distance that separates the substrate from the spray gun. Likewise, the highest adhesion force is at the spray velocity of 300 m/min, while we note that all the readings for powder coating are close and have a definite effect on the output. More precisely, the optimum adhesion strength can be obtained when the distance between the spray gun and the substrate is 250 mm, the powder feed rate is 15 g/min, the delay time is 4 minutes, and the spraying velocity is 300 m/min.

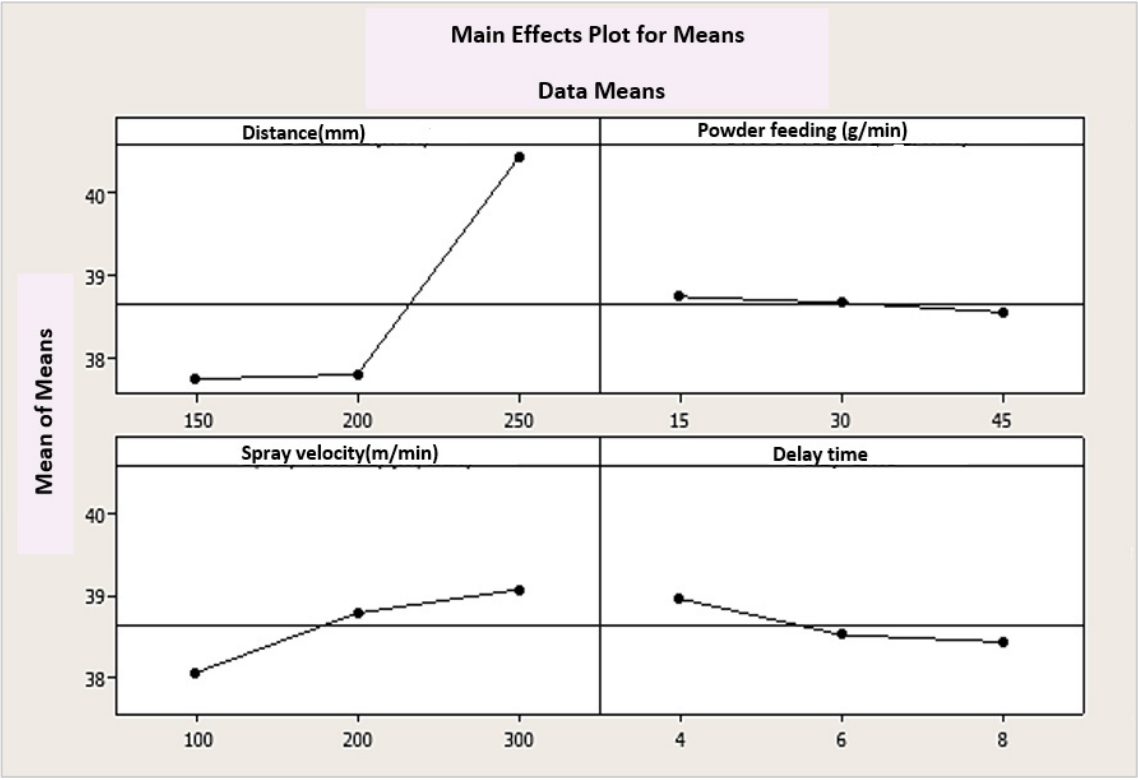

Figure 5: The main effect plot for the means

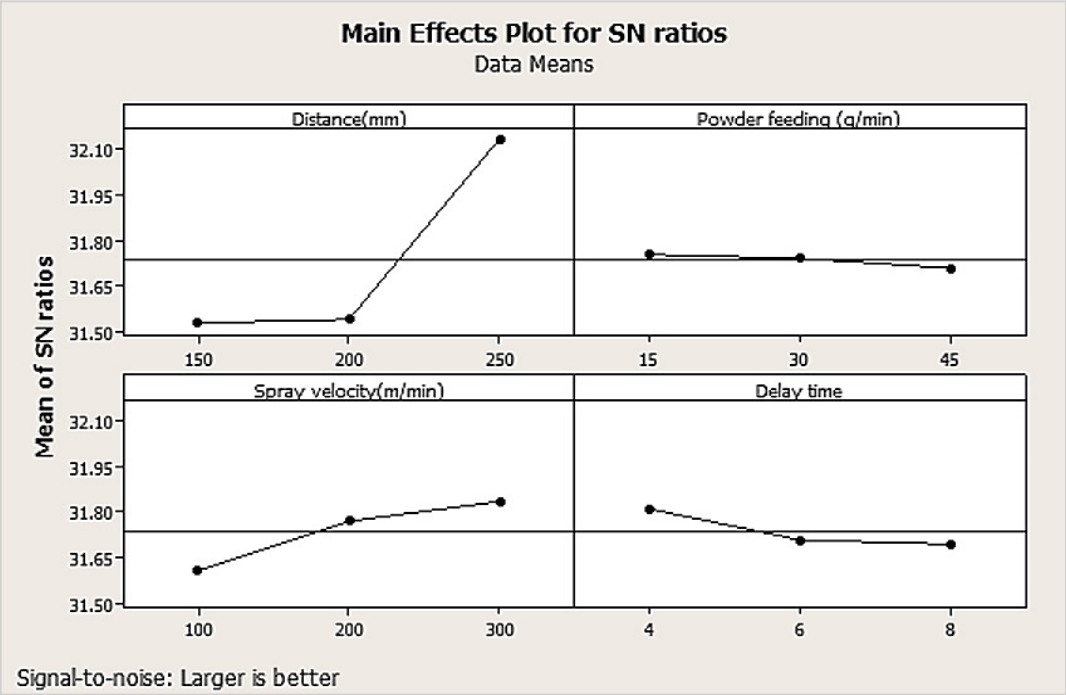

Figure 6: The main effect plot for the S/N Ratio

4.1 The adhesion strength analysis of variance (ANOVA)

Figure (7) illustrates that the considered parameters, including the distance between the gun spray and the substrate, the powder feeding, the spray velocity, the delay time, and their respective ranges, significantly affect the adhesion force between the Al metallic coating and the HDPE polymer substrate. ANOVA shows the effect of two factors on the outputs, and the amount of interaction between them measures the strength of the influence of the factors. We note a moderate interaction between distance and powder feeding at levels 2 and 3; the same is accurate between distance and spraying velocity and distance and delay time. Also, there is a strong interaction between powder feeding and spraying velocity and between powder feeding and delay time. Spray velocity and delay time. This means that the more the spray velocity is adjusted along with the powder feeding and the delay time, the more a homogeneous coating layer and a very high adhesion strength will be obtained.

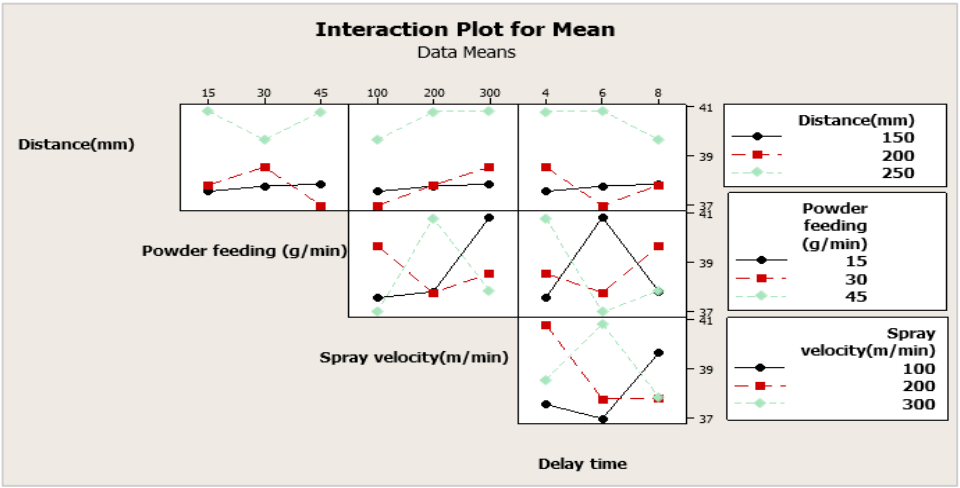

Figure 7: Interaction plot for the means

Figure (8a) demonstrates that the optimal adhesion force is found within the shaded area indicated by the dark green color, which exceeds 40N, across three distinct distances between the HDPE substrate, the spray gun, and the powder feeding. The optimal adhesion is attained when maintaining a distance of 240-250 mm between the substrate and the spray gun, accompanied by a feed rate of 40-45 g/min and a powder feeding rate of 15-20 g/min. Figure (8b) demonstrates that the optimal adhesion force is found within the shaded region indicated by the dark green color, which exceeds 40N. This observation is consistent across three levels of the distance between the HDPE substrate and the spray gun with varying spray velocities. The ideal adhesion is achieved when the distance between the substrate and the spray gun is maintained at 250 mm, with a spray velocity between 150 and 300 m/min. Figure (8c) illustrates that the optimal adhesion occurs at a distance of 250 mm between the HDPE polymer substrate and the aluminum metallic coating, with a delay time ranging from 4 to 7 minutes. Figure (8d) illustrates the effect of

the powder feeding and the delay time on the adhesion force. In particular, the optimal adhesion force occurs when the powder feeding rate is sustained within the 40-45 g/min range, accompanied by a delay time of 4 minutes. The powder feeding rate is established at 15 grams per minute, with a delay time ranging from 6 to 7 minutes. Figure (8e) illustrates the impact of the powder feeding and the spray velocity on the adhesion force between the HDPE substrate and the aluminum layer. The optimal adhesion force is attained at a powder feeding rate of 45 g/min, with a spray velocity between 150 and 250 m/min. The powder feeding rate can be 15g/min, with a corresponding spray velocity of 300m/min. Figure (8f) illustrates the relationship between the delay time and the spray velocity concerning the adhesion force between the HDPE substrate and the Al layer. The optimal adhesion force is attained with a delay time of 8 minutes and a spray velocity of 100 m/min, in addition to a delay time of 4 minutes with a spray velocity between 150 and 250 m/min. The achieved delay time ranges from 5 to 7 seconds, with a spray velocity of 300 m/min.

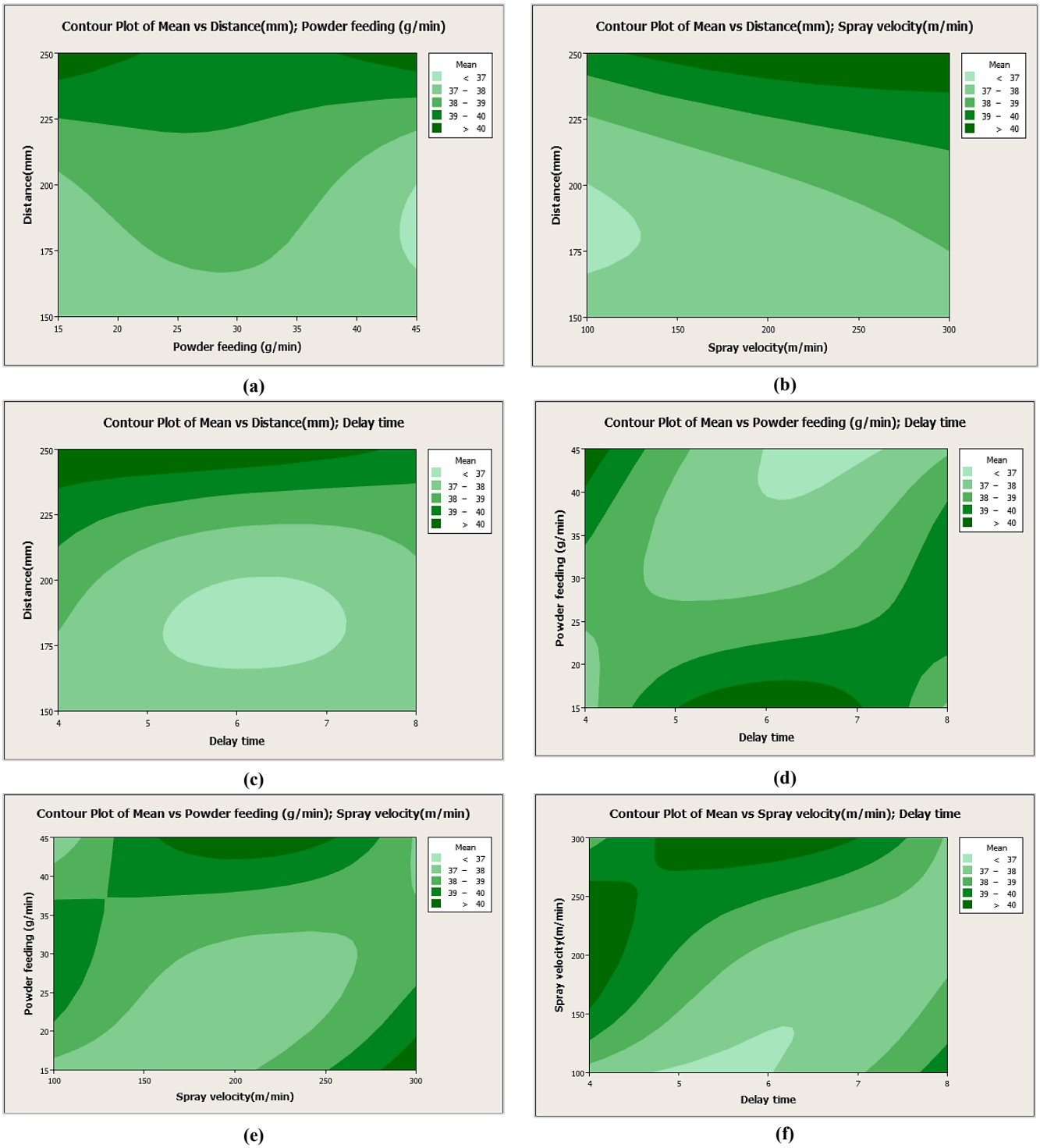

Figure 8: The contour plot for each of the two parameters**:** a) contour plot of mean vs distance (mm); powder feeding (g/min), b) contour plot of mean vs distance (mm); spray velocity (m/min), c) contour plot of mean vs distance (mm); delay time (min), d) contour plot of mean vs powder feeding(g/min); delay time (min), e) contour plot of mean vs powder feeding(g/min); spray velocity (m/min), f) contour plot of mean vs spray velocity (m/min); delay time (min)

4.2 Establishing the Predictive Model

The predictive model was created utilizing Minitab 17 for the comprehensive regression analysis, given that the experiments encompass several control factors (four control factors). General regression is a fundamental statistical analysis component that examines the relationship between control factors, their interactions, and the target response.

The equation presented below illustrates the regression model (2).

$$\text{Mean} = 33.303 + 0.027033\ (x) - 0.0063\ (y) + 0.005072\ (z) - 0.1322\ (g). \quad (2)$$

X is the distance between the spray gun and the substrate, y is the powder feed rate, z is the spraying velocity, and g is the delay time.

The data presented in Table (7) indicates that the distance between the substrate and the spray gun significantly impacts the adhesion strength, as evidenced by a P-value of (0.024).

Table 7: The regression results of the L9 orthogonal array for the adhesion strength

Term	Constant	Distance	Powder feeding	Spray velocity	Delay time
Coef	33.203	0.027033	-0.0063	0.005072	-0.1322
SE Coef	2.226	0.007673	0.02558	0.003837	0.1918
T-Value	14.92	3.52	-0.25	1.32	-0.69
P-Value	0	0.024	0.818	0.257	0.529

4.3 Optimal conditions and confirmation experiments

The optimal adhesion can be achieved under the conditions outlined in Table (8). The optimal design was not present in all trials of the L 9 orthogonal array of Table (4). In particular, the optimal value of the adhesion force was calculated using the formula presented in Table (8).

The optimal adhesion strength= A + B + C - 3 x (G. Mean) = 40.43+ 38.73+ 39.08+38.97 -3× (38.64) = 41.92

To achieve optimization, the practically optimum adhesion strength was determined based on experimental validation carried out under the optimal conditions, as outlined in Table (9).

Table 8: The optimal design condition

Factors	Distance	Powder Feeding	Spraying Velocity	Delay Time
Optimum Level	Level 3	Level 1	Level 3	Level 1

Table 9: Confirmation experiment under optimal conditions

Experiment Number	1	2	3
Distance (mm)	250	250	250
Powder Feed rate (g/min)	15	15	15
Spray Velocity (m/min)	300	300	4
Delay Time (min)	4	4	4
Predicted adhesion force	41.92	41.92	41.92
Exp. Adhesion force	42.56	43.451	43.312
Error%	1.5	3.5	3.21

5. Conclusion

This paper determined the optimal conduction of the thermal spray parameters to obtain the optimum adhesion strength of Al coatings on HDPE substrates. Specifically, the following points are the main findings of this work:

1) The surface of the uncoated HDPE sample was hydrophilic and had good wettability and adhesiveness, with a contact angle of 57.227°.
2) The optimal adhesion strength can be achieved if the distance between the spray gun and the substrate is 250 mm, the powder feeding rate is 15 g/min, the spray velocity is 300 m/min, and the delay period is 4min.
3) Optimal process variable values were utilized, resulting in strong concordance between experimental and predicted outcomes.
4) The Al layers were successfully deposited on the HDPE substrate without any degradation of the polymeric substrate due to the utilization of nanoparticles, which reduced the melting point. The Al nanoparticles were semi-molten before being automized on the polymeric substrate, and cooling air was used during the coating process.
5) The XRD X-ray diffraction showed no oxidation in the coating layer.
6) The aluminum layer showed a good electrical conductivity of ($2.08\times104\ \Omega^{-1}.cm^{-1}$). However, it is lower than that in bulk aluminum ($3.77\times105\ \Omega^{-1}.cm^{-1}$). This is because, due to a rise in grain boundaries, the resistance values were raised by the nanoparticles in the coating layer.

Author contributions

Conceptualization, G. Matrood, N. Abdulkader, and N. Ali; data curation, N. Abdulkader, and G. Matrood; formal analysis, G. Matrood, and N. Abdulkader; investigation, G. Matrood; methodology, N. Abdulkader; project administration, N. Abdulkader; resources, G. Matrood, and N. Abdulkader; software, G. Matrood; supervision, N. Abdulkader, and N. Ali; validation, G. Matrood, N. Abdulkader, and N. Ali; visualization, G. Matrood; writing—original draft preparation, G. Matrood; writing—review and editing, N. Abdulkader. All authors have read and agreed to the published version of the manuscript.

Funding

This research received no specific grant from any funding agency in the public, commercial, or not-for-profit sectors.

Data availability statement

The data supporting this study's findings are available on request from the corresponding author.

Conflicts of interest

The authors declare that there is no conflict of interest.

References

[1] J. T. Tsai, S. Akin, D. F. Bahr, and M. B.-G. Jun, A predictive modeling approach for cold spray metallization on polymers, Surf. Coat. Technol., 483 (2024) 130711. https://doi.org/10.1016/j.surfcoat.2024.130711

[2] A. Zhang, W. Wu, and D. Xie, Influence of laser treatment on the adhesion force of metallized carbon fiber reinforced polymer (CFRP) composite, Int. J. Adhes. Adhes., 135 (2024) 103830. https://doi.org/10.1016/j.ijadhadh.2024.103830

[3] H. Zhang, R. Xu, and T. Zhou, Selective Metallization of Thermoplastic Elastomers Based on Laser-Induced Surface Activation, Adv. Eng. Mater., 26 (2024) 2301715. https://doi.org/10.1002/adem.202301715

[4] Q. Duan and Y. Lu, Metallized liquid crystal polymer with low interfacial roughness and excellent adhesive strength based on semi-additive process for high-frequency signal transmission, Appl. Surf. Sci., 649 (2024) 159144. https://doi.org/10.1016/j.apsusc.2023.159144

[5] R. Melentiev, A. Yudhanto, R. Tao, T. Vuchkov, and G. Lubineau, Metallization of polymers and composites: State-of-the-art approaches, Mater. Des., 221 (2022) 110958. https://doi.org/10.1016/j.matdes.2022.110958

[6] F. Faupel, T. Strunskus, M. Kiene, A. Thran, C. Bechtolsheim, and V. Zaporojtchenko, Fundamental aspects of polymer metallization, MRS Online Proc. Lib., 511 (1998) 15-26. https://doi.org/10.1557/PROC-511-15

[7] Chiu, P. G., and D.T. Hsu, H.K. Kim, F.G. Shi, H.S. Nalwa. 2001. Chapter 6 - Low-k materials for microelectronics interconnects, In Handbook of Advanced Electronic and Photonic Materials and Devices, Vol. 4, pp. 201-234. Academic Press. https://doi.org/10.1016/B978-012513745-4/50041-X

[8] G. J. Matrood, A. M. Al-Gaban, and H. M. Yousif, Studying the Erosion Corrosion Behavior of NiCrAlY Coating Layer Applied on AISI 446 Stainless Steel Using Thermal Spray Technique, Eng. Technol. J., 38 (2020) 1676-1683. https://doi.org/10.30684/etj.v38i11A.1691

[9] P. Fauchais, G. Montavon, and G. Bertrand, From powders to thermally sprayed coatings, J. Therm. Spray Technol., 19 (2010) 56-80. https://doi.org/10.1007/s11666-009-9435-x

[10] V. Lakkannavar, K. Yogesha, C. D. Prasad, R. K. Phanden, G. Srinivasa, and S. C. Prasad, Thermal spray coatings on high-temperature oxidation and corrosion applications–a comprehensive review, Results Surf. Interfaces, 16 (2024) 100250. https://doi.org/10.1016/j.rsurfi.2024.100250

[11] G. M. Whitesides, Nanoscience, nanotechnology, and chemistry, Small, 1 (2005) 172-179. https://doi.org/10.1002/smll.200400130

[12] H. A. Akkar and S. Khalooq, Characteristics and evaluation of nano electronic devices, Eng. Technol. J., 32 (2014) 486-497. https://doi.org/10.30684/etj.32.3B.10

[13] D. R. Baer, J. E. Amonette, M. H. Engelhard, D. J. Gaspar, A. S. Karakoti, S. Kuchibhatla, and C. M. Wang, Characterization challenges for nanomaterials, Surf. Interface Anal., 40 (2008) 529-537. https://doi.org/10.1002/sia.2726

[14] T. A. Saleh, Properties of nanoadsorbents and adsorption mechanisms, Interface Sci. Technol., 34 (2022) 233-263. https://doi.org/10.1016/B978-0-12-849876-7.00010-5

[15] M. J. Meziani, C. E. Bunker, F. Lu, H. Li, W. Wang, E. A. Guliants, & Y. P. Sun, , Formation and properties of stabilized aluminum nanoparticles, ACS Appl. Mater. Interfaces, 1 (2009) 703-709. https://doi.org/10.1021/am800209m

[16] B. Medasani and I. Vasiliev, Computational study of the surface properties of aluminum nanoparticles, Surf. Sci., 603 (2009) 2042-2046. https://doi.org/10.1016/j.susc.2009.03.025

[17] B. Reeja-Jayan, P. Kovacik, R. Yang, A route towards sustainability through engineered polymeric interfaces, Adv. Mater. Interfaces, 1 (2014) 1400117. https://doi.org/10.1002/admi.201400117

[18] S. R. Jalal, Comparison OF Shear Properties for High Density Polyethylene (HDPE) and Poly vinyl Cloride (PVC) Polymers, Eng Technol. J., 33 (2015) 2039-2048. https://doi.org/10.30684/etj.2015.116222

[19] R.K. Roy, Design of Experiments Using Taguchi Approach: 16 Steps to Product and Process Improvement, Wiley, Hoboken, 2001, https://doi.org/10.1520/JTE12406JISBN 0-471-36101-1

[20] T. Ermergen and F. Taylan, Investigation of DOE model analyses for open atmosphere laser polishing of additively manufactured Ti-6Al-4V samples by using ANOVA, Opt. Laser Technol., 168 (2024) 109832. https://doi.org/10.1016/j.optlastec.2023.109832

[21] S.K. Madhavi, D. Sreeramulu, and M. Venkatesh, Evaluation of Optimum Turning Process of Process Parameters Using DOE andPCA Taguchi Method, Mater. Today, Proc., 4 (2017) 1937-1946. https://doi.org/10.1016/j.matpr.2017.02.039

[22] H.V. Pham, H.P. Nguyen, S. Shailesh, D.T. Nguyen, N.T. Bui, Investigating Technological Parameters and TiN-Coated Electrodes for Enhanced Efficiency in Ti-6Al-4V Micro-EDM Machining, Metals, 14 (2024) 1-13. https://doi.org/10.3390/met14020162

[23] B. Yelamasetti, M. Sandeep, S. Narella, V. Tiruchanur, T. Sonar, C. Prakash, & S. Kumar, Optimization of TIG welding process parameters using Taguchi technique for the joining of dissimilar metals of AA5083 and AA7075, Sci. Rep., 14 (2024) 23694. https://doi.org/10.1038/s41598-024-74458-6

[24] H. L. Alwan, B. M. Albaghdadi, M. M. AL-Khafaji, and A. A. Abbas, Estimation of cutting tool wear in turning using Taguchi method depending on weight of the removed tool metal, Eng. Technol. J., 32 (2014) 24-33. https://doi.org/10.30684/etj.32.1A.3

[25] J. Lu, L. Ni, S. Wang, and X. Mao, Grey-Taguchi analysis and experimental assessment of 1 GPa HSLA steel treated by quenching and tempering, J. Mater. Res. Technol., 29 (2024) 3508-3521. https://doi.org/10.1016/j.jmrt.2024.02.100

[26] S. Kulkarni and J. V. Gohel, Enhanced performance of perovskite solar cell by optimization of thin film control parameters using Taguchi method, Optik, p. 172090, 2024. https://doi.org/10.1016/j.ijleo.2024.172090

[27] J. Voyer, P. Schulz, and M. Schreiber, Electrically conductive flame sprayed aluminum coatings on textile substrates, J. Therm. Spray Technol., 17 (2008) 818-823. https://doi.org/10.1007/s11666-008-9228-7

[28] H. Ashrafizadeh, P. Mertiny, A. McDonald, Evaluation of the Influence of Flame Spraying Parameters on Microstructure and Electrical Conductivity of Al-12Si Coatings Deposited on Polyurethane Substrates, International Thermal Spray Conference, ASM International, 2015, 370-376. https://doi.org/10.31399/asm.cp.itsc2015p0370

[29] N. Huonnic, M. Abdelghani, P. Mertiny, and A. McDonald, Deposition and characterization of flame-sprayed aluminum on cured glass and basalt fiber-reinforced epoxy tubes, Surf. Coat. Technol., 205 (2010) 867-873. https://doi.org/10.1016/j.surfcoat.2010.08.029

[30] J. Affi, H. Okazaki, M. Yamada, and M. Fukumoto, Fabrication of aluminum coating onto CFRP substrate by cold spray, Mater. Trans., 52 (2011) 1759-1763. https://doi.org/10.2320/matertrans.T-M2011807

[31] A. J. Mohammed, H. A. Yousif, and S. S. Ahmed, Improving the deposition efficiency of the flame thermal spray coating process using ANOVA, in AIP Conf. Proc., 3105 (2024) AIP Publishing. https://doi.org/10.1063/5.0213307

[32] G. J. Matrood, N. J. Abdulkader, N. M. Ali, N.M., Study of behaviour and morphology of corrosion region of copper layer coated on polymer substrates by flame thermal spraying, International Information and Engineering Technology Association, Revue des Composites et des Matériaux Avancés-Journal of Composite and Advanced Materials, 34 (2024) 653-660. https://doi.org/10.18280/rcma.340513

[33] F. H. Edan, Prediction of Contact Angle for Sintered Alloy for Solid Freeform Fabrication, Eng Technol. J., 34 (2016) 1666-1672. http://dx.doi.org/10.30684/etj.34.8A.16

[34] N. X. Randall, The current state-of-the-art in scratch testing of coated systems, Surf. Coat. Technol., 380 (2019) 125092. https://doi.org/10.1016/j.surfcoat.2019.125092

[35] .J. Li and W. Beres, Scratch test for coating/substrate systems–A literature review, Can. Metall. Q., 46 (2007) 155-173 https://doi.org/10.1179/cmq.2007.46.2.155

[36] S. Bull and E. Berasetegui, An overview of the potential of quantitative coating adhesion measurement by scratch testing, Tribol. Int., 39 (2006) 99-114. https://doi.org/10.1016/j.triboint.2005.04.013

[37] M. Kalin and M. Polajnar, The correlation between the surface energy, the contact angle and the spreading parameter, and their relevance for the wetting behaviour of DLC with lubricating oils, Tribol. Int., 66 (2013) 225-233. https://doi.org/10.1016/j.triboint.2013.05.007

[38] A. A. AbdulRazak, Z. M. Shakor, and S. Rohani, Optimizing Biebrich Scarlet removal from water by magnetic zeolite 13X using response surface method, J. Environ. Chem. Eng., 6 (2018) 6175-6183. https://doi.org/10.1016/j.jece.2018.09.043

[39] L. Moraga, R. Henriquez, and B. Solis, Quantum theory of the effect of grain boundaries on the electrical conductivity of thin films and wires, Physica B: Condensed Matter, 470 (2015) 39-49. https://doi.org/10.1016/j.physb.2015.04.034